Improved Small-Signal Analysis for the Phase-Shifted PWM Power Converter

Michael J. Schutten, *Member, IEEE*, and David A. Torrey, *Member, IEEE*

***Abstract*—A closed form cycle by cycle analysis forms the basis for a new zero-voltage switching (ZVS) phase-shifted PWM (PSPWM) full bridge power converter small-signal model. The paper derives the small-signal response equations. The PSPWM converter has an implicit "slew interval," making the converter dynamics difficult to analyze using traditional averaging techniques. The converter control to output transfer function under continuous conduction mode operation and using voltage-mode control does not exhibit a second order pole associated with the output L-C filter, making it different from a conventional PWM converter. This new PSPWM converter model shows that the output L-C filter is separated into two real poles, with one pole held at constant frequency independent of operating conditions. A characteristic pole depends only upon the converter switching frequency and inductor values. This characteristic pole is fundamental to understanding the PSPWM converter natural and forced responses. The new small-signal model is shown to be in excellent agreement with experimental results.**

***Index Terms*—DC-DC power conversion, full-bridge converter, phase-shifted full bridge, phase-shifted pulse-width modulation, zero-voltage switching.**

I. Introduction

THE phase-shifted pulse-width modulated (PSPWM) full bridge dc to dc power converter is a popular topology due to its inherent electrical robustness and excellent electrical characteristics [1]–[3]. The converter uses zero-voltage switching (ZVS) to reduce switching loss, allowing high switching frequency operation and small energy storage components.

The PSPWM power converter using voltage mode control behaves differently from a conventional hard-switched buck converter. The PSPWM power converter duty cycle is a function of input voltage, output voltage, and load current. Thus, the PSPWM converter operating with a constant duty cycle and constant input voltage uniquely determines the output voltage only if load current is also specified. This has a significant impact upon the large-signal and small-signal characteristics of the PSPWM power converter.

The PSPWM power converter is in the "buck class," however the small-signal dynamics are different from a conventional hard-switched buck converter. The PSPWM converter control to output transfer function under continuous conduction mode using voltage-mode control does not exhibit a second order pole associated with the output L-C filter; this is in direct contrast to a hard-switched buck converter. There is a characteristic pole dependent upon the switching frequency, leakage inductor, and output inductor values. This pole is independent of operating conditions.

The large and small-signal operating characteristics of a phase-shifted PWM power converter are largely determined by the static and dynamic characteristics of the "slew interval." The slew interval is implicit to converter operation. The slew interval makes the converter dynamics and large-signal operation difficult to analyze. The PSPWM steady-state operating condition depends upon load current, further complicating the analysis.

The PSPWM converter slew interval is perturbed due to system disturbances (duty, v_{In}, v_{Out}, load current). During the slew interval the full input voltage (v_{In}) is applied across the leakage inductor (L_{Leak}). Increasing the load current increases the slew interval. The power delivery interval (for a constant duty cycle, D) decreases as load current increases, reducing the output voltage [4]. This unique operating characteristic, associated with the slew interval, contributes to the unconventional small-signal transfer functions of the PSPWM converter.

II. Large Signal Analysis

Fig. 1 shows the PSPWM power converter schematic. The following assumptions are used for analyzing the PSPWM power converter.

1) The switches (S1-S4) have zero on and infinite off resistance.
2) The switches (S1-S4) have negligible junction capacitance.
3) The rectifiers (R1-R4) have zero forward drop and zero junction capacitance.
4) Output voltage is constant over a switching cycle (small ripple voltage assumption).

It is important to emphasize that there is no small ripple assumption for either the leakage inductor current (I_{LLeak}) or the output inductor current (I_{LOut}). It is imperative to maintain these ac components to properly derive an accurate small-signal model [5]. When the PSPWM power converter load current is at the boundary of continuous conduction mode (i.e., I_{LOut} is always greater than zero) the peak-to-peak output inductor ripple is twice the level of its DC component. Ignoring these large ripple currents creates inaccuracies in the PSPWM power converter small-signal model.

The switching signals, control signals, and electrical waveforms are shown in Fig. 2. Fig. 3 displays the instantaneous

Manuscript received September 10, 2001; revised October 24, 2002. Recommended by Associate Editor K. Ngo.

M. J. Schutten is with the General Electric Global Research Center, Niskayuna, NY 12309 USA (e-mail: schutten@ieee.org).

D. A. Torrey is with the Advanced Energy Conversion, LLC, Ballston Spa, NY 12020 USA.

Digital Object Identifier 10.1109/TPEL.2003.809539

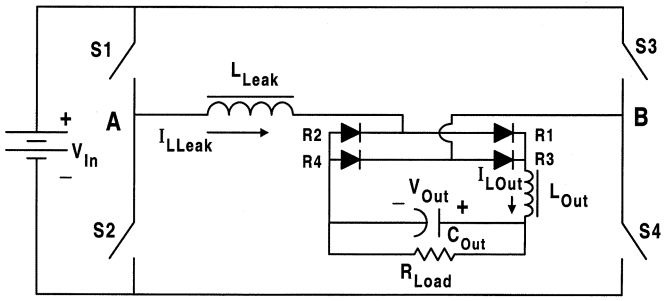

Fig. 1. Phase-shifted PWM power converter schematic.

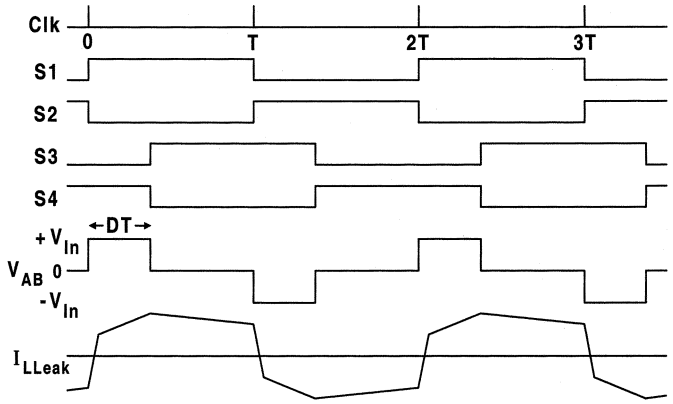

Fig. 2. PSPWM converter waveforms.

leakage and output inductor currents and voltages under steady-state operation. "DT" represents the controlled on-time of the switches. "ΓT" represents the slew interval. During the slew interval the leakage inductor current ramps from a value of $-I3$ until it clamps to the output inductor current value of $I1$. The slew interval is implicit to PSPWM converter operation, that is, there is no control command that determines the slew interval duration (ΓT): its length depends upon PSPWM converter operating conditions. The implicit slew interval complicates converter analysis. As load current increases the slew interval also increases. "T" is the system clock, corresponding to one-half of a complete full-bridge switching cycle.

The PSPWM converter is constrained to the output voltage ($V_{\rm Out}$) being smaller than the input voltage ($V_{\rm In}$). Thus, this converter is in the "buck classification" of power converters. Guidelines for designing this converter are to make the conversion ratio ($V_{\rm Out}/V_{\rm In}$) less than unity at the worst case operating condition of low input voltage and large load current.

The relationships between the currents in Fig. 3 are

$$I2 > I3 > I1 \tag{1}$$

since the output inductor current ($I_{\rm LOut}$) increases from $I1$ to $I2$ during time $(D-\Gamma)T$, then decreases from $I2$ to $I3$ during $(1-D)T$, and decreases from $I3$ to $I1$ during ΓT.

It is important to determine the criterion for maintaining continuous conduction mode (CCM) operation of the PSPWM power converter. CCM is defined as converter operation with the output inductor current ($I_{\rm LOut}$) always positive. CCM requires that the output inductor current cannot reach zero. $I_{\rm LOut}$ can never become negative due to the output diode bridge

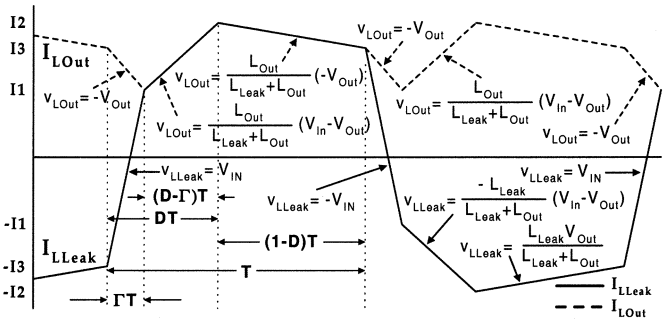

Fig. 3. Steady-state inductor current waveforms.

rectifier circuit. This CCM positive definite current requirement implies that during the slew interval (ΓT) the magnitude of the slope of $I_{\rm LOut}$ must be smaller than the magnitude of the slope of $I_{\rm LLeak}$. If this were not the case, the current $I_{\rm LOut}$ would reach zero during the ΓT interval in violation of CCM operation. Thus, a required condition for CCM operation is

$$\frac{V_{\rm In}}{L_{\rm Leak}} > \frac{V_{\rm Out}}{L_{\rm Out}}. \tag{2}$$

A. Inductor Current Analysis

The following equations provide the steady-state inductor current and duty cycle values of Fig. 3 [5]

$$I1 = \frac{\Gamma T}{2}\left(\frac{V_{\rm In}}{L_{\rm Leak}} - \frac{V_{\rm Out}}{L_{\rm Out}}\right) \tag{3}$$

$$I2 = \frac{\Gamma T}{2}\left(\frac{V_{\rm In}}{L_{\rm Leak}} + \frac{V_{\rm Out}}{L_{\rm Out}}\right) + \frac{V_{\rm Out}}{L_{\rm Leak}+L_{\rm Out}} \times (1-D)T \tag{4}$$

$$I3 = \frac{\Gamma T}{2}\left(\frac{V_{\rm In}}{L_{\rm Leak}} + \frac{V_{\rm Out}}{L_{\rm Out}}\right) \tag{5}$$

$$D = \frac{V_{\rm Out}}{V_{\rm In}} + \Gamma\left(1 + \frac{V_{\rm Out}}{V_{\rm In}}\frac{L_{\rm Leak}}{L_{\rm Out}}\right). \tag{6}$$

The average output inductor current is computed by averaging over a complete interval, T

$$\langle i_{\rm LOut}\rangle = \frac{1}{T}\int_t^{t+T} i_{\rm LOut}(\tau)d\tau = \left(\frac{D}{2}\right)I1 + \left(\frac{1}{2}-\frac{\Gamma}{2}\right)I2 + \left(\frac{1}{2}+\frac{\Gamma}{2}-\frac{D}{2}\right)I3. \tag{7}$$

Equation (7) relates the average output inductor current to currents $I1$, $I2$, and $I3$ of Fig. 3. The only additional required information is another independent relationship between the output voltage and output inductor current.

For the PSPWM converter, as well as any well-designed dc to dc converter, the output voltage ripple is much smaller than the dc voltage component. This means that the output voltage is well approximated by its dc component; this is the "small voltage ripple assumption" [6]. Using the small voltage ripple assumption, charge conservation, and steady-state operation gives

$$\langle i_{\rm LOut}\rangle = \frac{V_{\rm Out}}{R_{\rm Load}}. \tag{8}$$

Equation (8) requires all output inductor current, averaged over a complete switching cycle, to flow into the load resistor. If any net current flowed into or out of the output capacitor it would charge or discharge to a different voltage during the next switching cycle, violating the equilibrium assumption.

Substituting the output inductor current values $I1$, $I2$, and $I3$ into (7), replacing $\langle i_{\mathrm{LOut}} \rangle$ from (8), and simplifying gives the following important PSPWM converter equation

$$0 = \left(\frac{V_{\mathrm{Out}}}{V_{\mathrm{In}}} \frac{L_{\mathrm{Leak}}^2}{L_{\mathrm{Out}}^2} + \frac{L_{\mathrm{Leak}}}{L_{\mathrm{Out}}} \right) \Gamma^2 + \left(2 \frac{V_{\mathrm{Out}}}{V_{\mathrm{In}}} \frac{L_{\mathrm{Leak}}}{L_{\mathrm{Out}}} - \frac{L_{\mathrm{Leak}}}{L_{\mathrm{Out}}} - \frac{V_{\mathrm{In}}}{V_{\mathrm{Out}}} \frac{L_{\mathrm{Out}}}{L_{\mathrm{Leak}}} - \frac{V_{\mathrm{In}}}{V_{\mathrm{Out}}} + 1 \right) \Gamma + \left(\frac{V_{\mathrm{Out}}}{V_{\mathrm{In}}} - 1 + 2 \frac{L_{\mathrm{Leak}} + L_{\mathrm{Out}}}{T R_{\mathrm{Load}}} \right). \quad (9)$$

Equation (9) is a quadratic equation of the form

$$0 = a\Gamma^2 + b\Gamma + c \quad (10)$$

where there are in general two solutions. Only one of these solutions corresponds to the correct answer. Only the "subtraction quadratic solution" correctly maps increasing load current to an increasing slew interval (Γ). Thus, the solution of interest is

$$\Gamma = \frac{-b - \sqrt{b^2 - 4ac}}{2a}. \quad (11)$$

Another justification for (11) is this is the only solution that allows Γ to approach zero, a necessary operating condition for decreasing load current. The boundary condition for discontinuous conduction mode (output inductor current becomes zero) forces the slew interval (Γ) to approach zero.

B. Discontinuous Conduction Mode

For any power converter it is important to understand the boundary condition for discontinuous conduction mode (DCM) operation. DCM operation is defined as the output inductor current (I_{LOut}) reaching zero during the switching interval and staying at zero for a finite length of time. The PSPWM power converter DCM boundary condition occurs when the value of $I1$ is exactly zero. The only condition for which $I1$ equals zero is for the slew interval (Γ) to also equal zero. The a and $-b$ terms of (9) are always positive if $V_{\mathrm{In}} > V_{\mathrm{Out}}$ and $L_{\mathrm{Out}} > L_{\mathrm{Leak}}$ [5]. The requirement for Γ to be identically zero is the "c" term of (9) equaling zero. The critical resistance value for discontinuous conduction mode is

$$R_{\mathrm{DCM}} = \frac{2\{L_{\mathrm{Leak}} + L_{\mathrm{Out}}\}}{\left\{ T \left\{ 1 - \frac{V_{\mathrm{Out}}}{V_{\mathrm{In}}} \right\} \right\}}. \quad (12)$$

Any value of load resistance smaller than R_{DCM} ensures that the converter operates in continuous conduction mode. If the load resistor is larger than R_{DCM} the PSPWM power converter operates in discontinuous conduction mode.

III. Small Signal Analysis

The closed form large-signal operating conditions provide the operating point for small-signal operation. The PSPWM converter load characteristics require input voltage (V_{In}), output voltage (V_{Out}), and load (R_{Load}) to uniquely specify the duty cycle (D). This is different from a buck converter where specifying the input voltage and output voltage determines the duty cycle (in continuous conduction mode).

The PSPWM converter using voltage mode control has a slew interval (ΓT) perturbation when any other parameter is perturbed. There is no dual of the slew interval in the buck converter. If the PSPWM converter input voltage is perturbed, the output voltage will reach a new steady state value dependent upon load current (assuming duty and load are constant), and the slew interval responds appropriately. This creates different PSPWM converter small-signal dynamics.

A. PSPWM Power Converter Natural Response

The natural response of a system is the dynamic behavior of a perturbed system returning back to steady-state operation. For the phase-shifted PWM power converter the perturbed output parameter of interest is the output inductor current (i_{LOut}). The PSPWM power converter has a natural response characteristic similar to a sampled data system. The natural response of the small-signal output inductor current (Δi_{LOut}) remains constant for a half switching cycle (T). The magnitude then reduces by a constant ratio during the small-signal slew interval.

The PSPWM power converter slew interval is perturbed by any input disturbance (Δv_{In}, Δv_{Out}, Δd). A small-signal input perturbation causes a small-signal output inductor current (Δi_{LOut}) perturbation.

Fig. 4 shows the output inductor current and leakage inductor current under steady-state ($I_{\mathrm{LOut}}, I_{\mathrm{LLeak}}$) and perturbed ($I_{\mathrm{LOut}} + \Delta i_{\mathrm{LOut}}$, $I_{\mathrm{LLeak}} + \Delta i_{\mathrm{LLeak}}$) operating conditions. The inductor currents are perturbed, but no additional external disturbance or perturbation is introduced. The input voltage, V_{In}, output voltage, V_{Out}, and duty cycle, D, are all unperturbed. The magnitude of the output inductor current perturbation is Δi_{LOut}. The perturbation magnitude is the same for the output inductor current and leakage inductor current, since previous to DT the output and leakage inductors are connected in series through the output bridge rectifier [7]. The output and leakage inductor currents are the negatives of each other due to the conduction of bridge rectifiers R2 and R3 of Fig. 1.

A perturbation of output and leakage inductor currents with magnitude Δi_{LOut} exists just before DT. Before DT the steady-state and perturbed output inductor currents are each rising with a slope of $(V_{\mathrm{In}} - V_{\mathrm{Out}})/(L_{\mathrm{Out}} + \mathrm{L}_{\mathrm{Leak}})$ and the steady-state and perturbed leakage inductor currents are falling with a slope of $-(V_{\mathrm{In}} - V_{\mathrm{Out}})/(L_{\mathrm{Out}} + \mathrm{L}_{\mathrm{Leak}})$. Between times ($DT$, T) and (T, $T + \Gamma T$) the perturbed output inductor current slope is the same as the steady-state output inductor current slope, similarly the perturbed leakage inductor current slope is the same as the steady-state leakage inductor current slope. Until time T the perturbed output inductor current ($I_{\mathrm{LOut}} + \Delta i_{\mathrm{LOut}}$) and leakage inductor current ($I_{\mathrm{LLeak}} + \Delta i_{\mathrm{LLeak}}$) have equal magnitudes, but the perturbed leakage inductor current is the negative of the perturbed output inductor current due to the conduction of the bridge rectifier diodes. The magnitude of the output inductor current and leakage inductor current perturbations each remains constant at Δi_{LOut} until time $T + \Gamma T$. The perturbed output and leakage inductor currents at time $T + \Gamma T$ differ by $2\Delta i_{\mathrm{LOut}}$. The

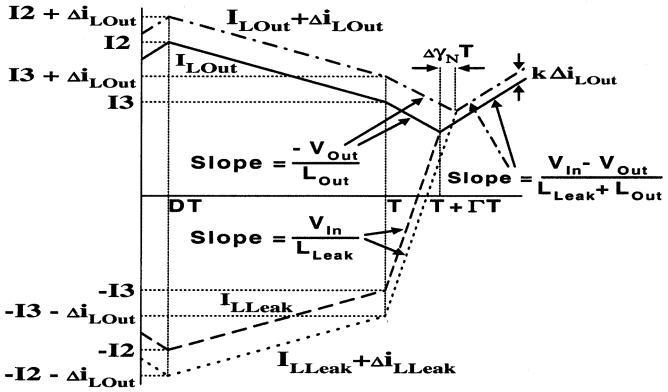

Fig. 4. Steady-state and perturbed currents ($V_{\rm In}$, $V_{\rm Out}$, D unperturbed).

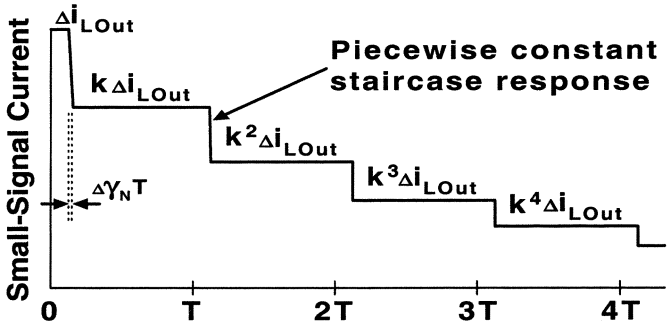

Fig. 5. Characteristic staircase natural response for the PSPWM converter.

perturbed output inductor current continues to fall with a slope of $-V_{\rm Out}/L_{\rm Out}$, and the perturbed leakage inductor current continues to rise with a slope of $V_{\rm In}/L_{\rm Leak}$. At the end of the perturbed slew interval, $T+\Gamma T+\Delta\gamma_N T$, the perturbed output inductor current and perturbed leakage inductor current are again equal since they are connected in series by rectifier diodes R1 and R4 of Fig. 1. Since the inductors are again connected in series they must have the same perturbation value, $k\Delta i_{\rm LOut}$. The corresponding small-signal slew interval ($\Delta\gamma_N T$) is a characteristic of the PSPWM converter.

Solving the small-signal slew interval using the geometry of Fig. 4 gives

$$\Delta\gamma_N T=\frac{2L_{\rm Leak}L_{\rm Out}}{V_{\rm Out}L_{\rm Leak}+V_{\rm In}L_{\rm Out}}\Delta i_{\rm LOut}. \tag{13}$$

The length of this slew interval perturbation depends upon the magnitude of the small-signal inductor current perturbation ($\Delta i_{\rm LOut}$) at time T (or at $T+\Gamma T$), the steady-state converter voltages ($V_{\rm In}, V_{\rm Out}$), and inductances ($L_{\rm Leak}, L_{\rm Out}$).

There is a rapid change in the small-signal output inductor current during the small-signal slew interval ($\Delta\gamma_N T$), as shown in Fig. 5. The output inductor current perturbation stays constant with a value of $\Delta i_{\rm LOut}$ until time ΓT. At time $\Gamma T+\Delta\gamma_N T$ the small-signal output inductor current is a different constant value. During the small-signal slew interval ($\Delta\gamma_N T$) the small-signal output inductor current ramps between a constant value and a different constant value.

The slopes of the steady-state and perturbed output inductor currents in Fig. 4 are identical before time $T+\Gamma T$ since the input voltage ($V_{\rm In}$), output voltage ($V_{\rm Out}$), and inductor values are the same for both cases. Similarly, the slopes of the steady-state and perturbed output inductor currents are again equal after time $T+\Gamma T+\Delta\gamma_N T$. The small-signal output inductor current ($\Delta i_{\rm LOut}$) of Fig. 4 changes its value at the end of the perturbed slew interval ($T+\Gamma T+\Delta\gamma_N T$) by

$$k\Delta i_{\rm LOut}=\Delta i_{\rm LOut}-\frac{V_{\rm Out}}{L_{\rm Out}}\Delta\gamma_N T-\frac{V_{\rm In}-V_{\rm Out}}{L_{\rm Leak}+L_{\rm Out}}\Delta\gamma_N T. \tag{14}$$

Substituting the value of $\Delta\gamma_N T$ from (13) and solving for k gives

$$k=\frac{L_{\rm Out}-L_{\rm Leak}}{L_{\rm Out}+L_{\rm Leak}}. \tag{15}$$

The value of k is constrained between zero and one, since $0<L_{\rm Leak}<L_{\rm Out}$.

The small-signal output inductor current of each successive time interval reduces by a factor dependent upon the output and leakage inductances. This new perturbation value is held constant for a half-cycle switching interval, T (minus the small-signal slew interval, $\Delta\gamma_N T$), then reduces by a factor of k. This new level is constant until the next slew interval perturbation, then reduces by another factor of k. Thus, the inductance values ($L_{\rm Leak}, L_{\rm Out}$) and the switching interval (T) determine the PSPWM power converter natural response.

The PSPWM converter natural response is

$$\Delta i_{\rm LOut}(NT)=k^N\Delta i_{\rm LOut}(0) \tag{16}$$

where N is a positive integer corresponding to the number of half-cycle switching intervals since the small-signal inductor current perturbation was introduced.

The characteristic value "k" corresponds to the PSPWM power converter natural response. The output inductor current perturbation ($\Delta i_{\rm LOut}$) relaxes back toward its steady-state operating condition with the characteristic staircase ramp pattern shown in Fig. 5, where the small-signal output inductor current perturbation ($\Delta i_{\rm LOut}$) was introduced at time zero. The time interval T corresponds to one-half of a switching period. Each successive time interval has the perturbation magnitude reduced by a factor of "k." The value of k in Fig. 5 is approximately 3/4 (or $L_{\rm Out}\cong 6L_{\rm Leak}$). The slope associated with the piecewise constant staircase fall time is very large. The amplitude change occurs during the small-signal slew interval, $\Delta\gamma_N T$. The small-signal slew interval decreases toward zero as the small-signal output inductor current returns toward steady-state with increasing switching cycles.

B. PSPWM Power Converter Complete Response

The PSPWM converter forced response is its dynamic response due to external disturbances. The PSPWM power converter disturbances are input voltage ($v_{\rm In}$), output voltage ($v_{\rm Out}$), and duty cycle (d).

The small-signal model uses unit step input perturbations that occur at time zero. The small-signal inputs are duty cycle perturbation, $\Delta d u(t)$, input voltage perturbation, $\Delta v_{\rm In}u(t)$, and output voltage perturbation, $\Delta v_{\rm Out}u(t)$. To simplify the equations the unit step function, $u(t)$, is not explicitly included in the equations. The unit step perturbations of duty cycle, input voltage, and output voltage are presented as Δd, $\Delta v_{\rm In}$, and $\Delta v_{\rm Out}$, respectively.

The important small-signal transfer functions for characterizing the PSPWM power converter are control to output ($\Delta v_{\rm Out}/\Delta d$), audio susceptibility (or input to output voltage, $\Delta v_{\rm Out}/\Delta v_{\rm In}$), output impedance ($\Delta v_{\rm Out}/\Delta i_{\rm Out}$), and input impedance ($\Delta v_{\rm In}/\Delta i_{\rm In}$). These transfer functions provide the necessary information for deriving the important PSPWM converter small-signal model. The small-signal slew interval ($\Delta\gamma_{\rm NF}$) response is a necessary intermediate parameter to develop the PSPWM power converter small-signal transfer functions.

The small-signal model is derived from perturbing the PSPWM power converter steady-state operation. Proper converter modeling requires understanding slew interval dynamics associated with the natural and forced responses. The slew interval is implicit to the converter operation. There is no switching event or control operation causing the end of the slew interval. This is different from classical PWM power converters where the duty cycle begins when a switch is explicitly turned on and ends when the controlled switch is turned off.

The PSPWM power converter dynamics are determined by the system response while transitioning between one operating condition and a different operating condition. The PSPWM converter dynamics result from the combination of natural and forced responses. Fig. 6 shows the PSPWM converter leakage and output inductor currents under steady-state and perturbed operating conditions. The time scale is expanded to demonstrate slew interval operation under steady-state and perturbed operating conditions. The perturbed output inductor current at time 0 has a value of $I3 + \Delta i_{\rm LOut:0}$. The perturbed leakage inductor current at time 0 is $-I3 - \Delta i_{\rm LOut:0}$, since the leakage inductor was in series with the negative of the output inductor at time 0^- (i.e., just before time 0).

The small-signal output inductor current of Fig. 6 has a nonzero value of $\Delta i_{\rm LOut:0}$ at time zero. This is the instantaneous difference between the perturbed and steady-state output inductor currents. The terminology for the small-signal output inductor current is

$$\Delta i_{\rm LOut:0} \equiv \Delta i_{\rm LOut}(0). \tag{17}$$

Small-signal input voltage and output voltage perturbations ($\Delta v_{\rm In}, \Delta v_{\rm Out}$) also exist at time 0. Since the output inductor and leakage inductors were connected in series (through the output bridge rectifier) before time 0, the perturbation of $-\Delta i_{\rm LOut:0}$ must be also added to the leakage inductor current. The input and output voltages are perturbed to $V_{\rm In} + \Delta v_{\rm In}$ and $V_{\rm Out} + \Delta v_{\rm Out}$, respectively. The perturbed output inductor and leakage inductor currents result in a small-signal slew interval ($\Delta\gamma_{\rm NF}T$) component. The perturbed slew interval is $\Gamma T + \Delta\gamma_{\rm NF}T$. The subscript "NF" denotes that the perturbation is due to both the natural response ($\Delta i_{\rm LOut:0}$) and forced responses ($\Delta v_{\rm In}, \Delta v_{\rm Out}$). Solving for the small-signal slew interval using the geometry of Fig. 6 gives

$$\Delta\gamma_{\rm NF}T = \frac{2L_{\rm Leak}L_{\rm Out}\Delta i_{\rm LOut:0} - \Gamma T L_{\rm Out}\Delta v_{\rm In} - \Gamma T L_{\rm Leak}\Delta v_{\rm Out}}{V_{\rm Out}L_{\rm Leak} + V_{\rm In}L_{\rm Out}}. \tag{18}$$

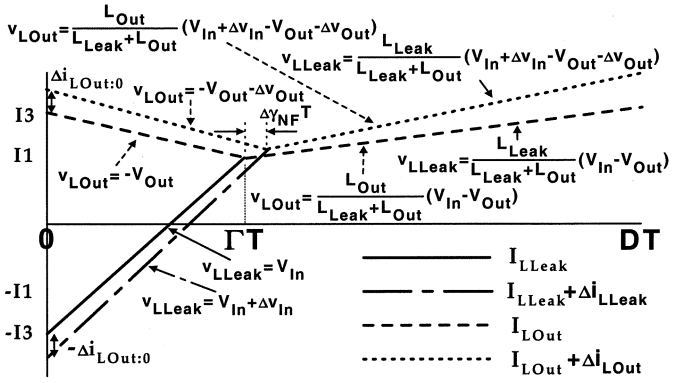

Fig. 6. Steady-state and perturbed output and leakage inductor currents.

Equation (18) provides a tremendous amount of physical insight into the phase-shifted PWM power converter small-signal dynamics. The small-signal slew interval depends upon the inductor values ($L_{\rm Leak}$ and $L_{\rm Out}$), the steady-state operating conditions ($V_{\rm Out}$, $V_{\rm In}$, T, and Γ), the small-signal output inductor current at the beginning of the half-switching cycle ($\Delta i_{\rm LOut:0}$), and the input and output voltage perturbations ($\Delta v_{\rm In}$ and $\Delta v_{\rm Out}$). Positive current perturbations ($\Delta i_{\rm LOut:0} > 0$) increase the slew interval. Positive input voltage or output voltage perturbations ($\Delta v_{\rm In}, \Delta v_{\rm Out}$) decrease the slew interval. The small-signal slew interval provides damping for the output L-C filter [4].

Duty cycle perturbations (ΔdT) are not explicitly included in (18). Any small-signal duty perturbation occurs after the perturbed slew interval ($\Gamma T + \Delta\gamma_{\rm NF}T$) has ended. The output inductor current and leakage inductor current are updated at the end of each half switching cycle to include the effect of duty cycle (ΔdT) perturbations. The small-signal slew interval ($\Delta\gamma_{\rm NF}T$) dependence upon duty cycle perturbations (ΔdT) is included by its effect upon the small-signal output inductor current at the beginning of the next switching interval ($\Delta i_{{\rm LOut:}T}$).

C. Output Inductor Current Small-Signal Response

Time evolution of the small-signal output inductor current provides dynamic information necessary to derive the PSPWM power converter small-signal model. The small-signal output inductor current is an important parameter since all load current and output capacitor current must flow through the output inductor.

From the steady-state and the perturbed output inductor currents of Fig. 7 it is possible to derive the time evolution of the perturbed output inductor current. The generalized response calculates the perturbed output inductor current due to a small-signal current perturbation ($\Delta i_{\rm LOut:0}$), small-signal output voltage perturbation ($\Delta v_{\rm Out}$), small-signal input voltage perturbation ($\Delta v_{\rm In}$), and small-signal duty cycle perturbation (ΔdT).

The perturbed output inductor current can be calculated by projecting forward in time. The steady-state output inductor current has a value of $I3$ at time zero, $I1$ at time ΓT, and $I2$ at time DT. The perturbed output inductor current is $I3 + \Delta i_{\rm LOut:0}$ at time zero.

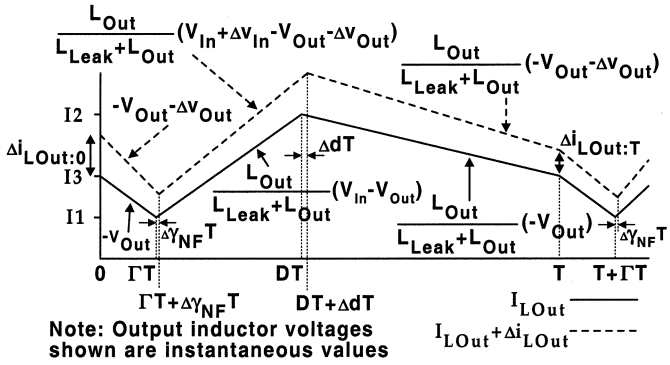

Fig. 7. Steady-state and perturbed output inductor currents.

The perturbed output inductor current at time ΓT is solved using the perturbed output inductor current at time zero of Fig. 7 and projecting forward in time to ΓT

$$\begin{aligned} I_{\mathrm{LOut}}(\Gamma T)+\Delta i_{\mathrm{LOut}}(\Gamma T) &= I_{\mathrm{LOut}}(0)+\Delta i_{\mathrm{LOut:0}}-\frac{V_{\mathrm{Out}}+\Delta v_{\mathrm{Out}}}{L_{\mathrm{Out}}}\Gamma T \\ &= I3-\frac{V_{\mathrm{Out}}}{L_{\mathrm{Out}}}\Gamma T-\frac{\Delta v_{\mathrm{Out}}}{L_{\mathrm{Out}}}\Gamma T+\Delta i_{\mathrm{LOut:0}} \\ &= I1+\Delta i_{\mathrm{LOut:0}}-\frac{\Delta v_{\mathrm{Out}}}{L_{\mathrm{Out}}}\Gamma T. \end{aligned} \tag{19}$$

The small-signal output inductor current is the difference between the perturbed and steady-state output inductor currents. The steady-state output inductor current is $I1$ at ΓT. The small-signal output inductor current at ΓT is

$$\Delta i_{\mathrm{LOut}}(\Gamma T)=\Delta i_{\mathrm{LOut:0}}-\frac{\Gamma T}{L_{\mathrm{Out}}}\Delta v_{\mathrm{Out}}. \tag{20}$$

Similarly solving the small-signal output inductor current at all the other times of interest gives [5]

$$\Delta i_{\mathrm{LOut}}(\Gamma T+\Delta\gamma_{\mathrm{NF}}T)= k\Delta i_{\mathrm{LOut:0}}+\frac{\Gamma T\{\Delta v_{\mathrm{In}}-\Delta v_{\mathrm{Out}}\}}{L_{\mathrm{Leak}}+L_{\mathrm{Out}}} \tag{21}$$

$$\Delta i_{\mathrm{LOut}}(DT)= k\Delta i_{\mathrm{LOut:0}}+\frac{DT\{\Delta v_{\mathrm{In}}-\Delta v_{\mathrm{Out}}\}}{L_{\mathrm{Leak}}+L_{\mathrm{Out}}} \tag{22}$$

$$\Delta i_{\mathrm{LOut}}(DT+\Delta dT)= k\Delta i_{\mathrm{LOut:0}}+\frac{DT\{\Delta v_{\mathrm{In}}-\Delta v_{\mathrm{Out}}\}+V_{\mathrm{In}}\Delta dT}{L_{\mathrm{Leak}}+L_{\mathrm{Out}}} \tag{23}$$

$$\Delta i_{\mathrm{LOut}}(T)\equiv\Delta i_{\mathrm{LOut:}T}= k\Delta i_{\mathrm{LOut:0}}+\frac{DT\Delta v_{\mathrm{In}}-T\Delta v_{\mathrm{Out}}+V_{\mathrm{In}}\Delta dT}{L_{\mathrm{Leak}}+L_{\mathrm{Out}}}. \tag{24}$$

D. Generalized Small-Signal Output Inductor Current

Equations (20)–(24) provide the small-signal output inductor current response during the first switching interval after the unit step input perturbations. The small-signal output inductor current is not zero at time zero ($\Delta i_{\mathrm{LOut:0}}\neq 0$) when the unit step input perturbation begins. The generalized small-signal response solves the instantaneous small-signal output inductor current for all input perturbations; $\Delta i_{\mathrm{LOut:0}}$, Δv_{In}, Δv_{Out}, ΔdT.

The small-signal model requires input perturbations to be introduced after the PSPWM converter has reached steady-state operation. The small-signal output inductor current is solved for all times after introduction of the small-signal unit step input perturbations. Unit step input perturbations are introduced at an arbitrary time "zero," corresponding to the beginning of a PSPWM power converter switching interval.

The method of calculating the small-signal response assumes PSPWM power converter steady-state operation before time zero. Thus, there is no small-signal output inductor current at time zero ($\Delta i_{\mathrm{LOut:0}}=0$). A unit step input perturbation begins at time zero, and the resultant converter small-signal output inductor response is calculated using (20)–(24). The small-signal output inductor current at time T is used as the new starting value in (17) and represented as $\Delta i_{\mathrm{LOut:}T}$. Equations (20)–(24) are again used to determine the small-signal output inductor currents between times T and $2T$. This process is then repeated for the next switching interval, $2T$ to $3T$, and so on. This response is generalized for any time after the perturbation was introduced. The resulting equations have the form of a geometric progression. This simplifies the small-signal equations. The final generalized small-signal output inductor current during switching interval "N" after the introduction of a unit step input perturbation is

$$\Delta i_{\mathrm{LOut}}(NT)= \frac{1-k^N}{2L_{\mathrm{Leak}}}\{DT\Delta v_{\mathrm{In}}-T\Delta v_{\mathrm{Out}}+V_{\mathrm{In}}\Delta dT\} \tag{25}$$

$$\Delta i_{\mathrm{LOut}}(NT+\Gamma T)= \frac{1-k^N}{2L_{\mathrm{Leak}}}\{DT\Delta v_{\mathrm{In}}-T\Delta v_{\mathrm{Out}}+V_{\mathrm{In}}\Delta dT\}-\frac{\Gamma T}{L_{\mathrm{Out}}}\Delta v_{\mathrm{Out}} \tag{26}$$

$$\Delta i_{\mathrm{LOut}}(NT+\Gamma T+\Delta\gamma_{\mathrm{NF}}T)= k\frac{1-k^N}{2L_{\mathrm{Leak}}}\{DT\Delta v_{\mathrm{In}}-T\Delta v_{\mathrm{Out}}+V_{\mathrm{In}}\Delta dT\}+\frac{\Gamma T\{\Delta v_{\mathrm{In}}-\Delta v_{\mathrm{Out}}\}}{L_{\mathrm{Leak}}+L_{\mathrm{Out}}} \tag{27}$$

$$\Delta i_{\mathrm{LOut}}(NT+DT)= k\frac{1-k^N}{2L_{\mathrm{Leak}}}\{DT\Delta v_{\mathrm{In}}-T\Delta v_{\mathrm{Out}}+V_{\mathrm{In}}\Delta dT\}+\frac{DT\{\Delta v_{\mathrm{In}}-\Delta v_{\mathrm{Out}}\}}{L_{\mathrm{Leak}}+L_{\mathrm{Out}}} \tag{28}$$

$$\Delta i_{\mathrm{LOut}}(NT+DT+\Delta dT)= k\tfrac{1-k^N}{2L_{\mathrm{Leak}}}\{DT\Delta v_{\mathrm{In}}-T\Delta v_{\mathrm{Out}}+V_{\mathrm{In}}\Delta dT\}+\frac{DT\{\Delta v_{\mathrm{In}}-\Delta v_{\mathrm{Out}}\}+V_{\mathrm{In}}\Delta dT}{L_{\mathrm{Leak}}+L_{\mathrm{Out}}} \tag{29}$$

$$\Delta i_{\mathrm{LOut}}(NT+T)= \frac{1-k^{N+1}}{2L_{\mathrm{Leak}}}\{DT\Delta v_{\mathrm{In}}-T\Delta v_{\mathrm{Out}}+V_{\mathrm{In}}\Delta dT\}. \tag{30}$$

E. Averaged Small-Signal Response

The technique to derive the PSPWM power converter small-signal model is now summarized to clarify the averaging approach. The averaging process used in this paper begins with the exact small-signal output inductor currents at each subinterval from (25)–(30). The first step involves averaging these subinterval equations over one complete (half) switching interval, T. This linearization process provides a first order discrete sampled data equation. All resulting coefficients in the cycle by cycle averaged (32) are simple constants except the $1-k^N$ term. Equation (32) is a first order discrete time staircase response with amplitude step changes occurring at the beginning of successive switching intervals. The next step is to perform a Laplace transform on the averaged first order sampled equation. The resulting Laplace equation includes a complicating "e^{-sT}" term. The final step uses a Pade approximation to simplify the s-domain averaged small-signal equation to a simple pole-zero form.

Equations (25)–(30) provide information for calculating the PSPWM power converter small-signal model. It is important to understand the averaging process. The averaging interval is one complete (half) switching cycle, beginning and ending at the system clock. Thus, the first averaging interval is from 0 to T, the next from T to $2T$, and so on. The averaged small-signal output inductor current exhibits a "step change" in amplitude at the beginning of each half-cycle switching cycle. The value stays constant until the next half-cycle switching interval. This averaged value during a switching interval is exactly the same as the average of the exact model. This averaging approach provides a basis for developing the PSPWM power converter small-signal model.

The averaging technique uses the exact small-signal equations of (25)–(30). The exact small-signal output inductor current response is known at each time interval. The averaged small-signal output inductor current is evaluated by averaging the exact small-signal output inductor current equations over one complete switching interval. For the Nth cycle after the perturbation is introduced the averaged value is

$$\begin{aligned}
&\Delta\langle i_{\mathrm{LOut}}(t)\rangle_N \\
&\equiv\frac{1}{T}\int_{NT}^{NT+T}\Delta i_{\mathrm{LOut}}(\tau)d\tau \\
&=\frac{1}{T}\left\{\frac{\Delta i_{\mathrm{LOut}}(NT)+\Delta i_{\mathrm{LOut}}(NT+\Gamma T)}{2}\Gamma T\right. \\
&\quad+\frac{\Delta i_{\mathrm{LOut}}(NT+\Gamma T)+\Delta i_{\mathrm{LOut}}(NT+\Gamma T+\Delta\gamma_{\mathrm{NF}}T)}{2} \\
&\quad\times\Delta\gamma_{\mathrm{NF}}T \\
&\quad+\frac{\Delta i_{\mathrm{LOut}}(NT+\Gamma T+\Delta\gamma_{\mathrm{NF}}T)+\Delta i_{\mathrm{LOut}}(NT+DT)}{2} \\
&\quad\times\{DT-\{\Gamma T+\Delta\gamma_{\mathrm{NF}}T\}\} \\
&\quad+\frac{\Delta i_{\mathrm{LOut}}(NT+DT)+\Delta i_{\mathrm{LOut}}(NT+DT+\Delta dT)}{2}\Delta dT \\
&\quad+\frac{\Delta i_{\mathrm{LOut}}(NT+DT+\Delta dT)+\Delta i_{\mathrm{LOut}}(NT+T)}{2} \\
&\quad\left.\times\{T-\{DT+\Delta dT\}\}\right\}.
\end{aligned} \tag{31}$$

Putting the values from (25)–(30) into (31), simplifying, and ignoring terms that are the product of two small-signal values [6] gives

$$\begin{aligned}
\Delta\langle i_{\mathrm{LOut}}\rangle_N =&\frac{T}{2L_{\mathrm{Leak}}}\left\{(1-k^N)(k+\Gamma-k\Gamma)\right. \\
&\left.+\frac{1-k}{2}\left(1+\Gamma^2\frac{L_{\mathrm{Leak}}}{L_{\mathrm{Out}}}\right)\right\} \\
&\times\{D\Delta v_{\mathrm{In}}-\Delta v_{\mathrm{Out}}+V_{\mathrm{In}}\Delta d\}+\frac{T}{2L_{\mathrm{Leak}}}\frac{1-k}{2} \\
&\times\left\{\left(1-D-\frac{\Gamma^2}{D}-\Gamma^2\frac{L_{\mathrm{Leak}}}{L_{\mathrm{Out}}}\right)D\Delta v_{\mathrm{In}}\right. \\
&\left.+\left(1-2D-\Gamma^2\frac{L_{\mathrm{Leak}}}{L_{\mathrm{Out}}}\right)V_{\mathrm{In}}\Delta d\right\}.
\end{aligned} \tag{32}$$

Equation (32) is the important PSPWM power converter averaged small-signal output inductor equation. This provides the exact averaged small-signal output inductor current response due to small-signal inputs. The resulting small-signal model uses the dc operating conditions ($D, V_{\mathrm{In}}, \Gamma$) and the PSPWM power converter component parameters ($L_{\mathrm{Leak}}, L_{\mathrm{Out}}, k, T$). The output voltage ($V_{\mathrm{Out}}$) is implicitly included from the dc duty ratio (D). The input perturbations are $\Delta v_{\mathrm{In}}u(t)$, $\Delta v_{\mathrm{Out}}u(t)$, $\Delta du(t)$. All coefficients in (32) are constant, except the important "$1-k^N$" term. This term provides the characteristic staircase pattern that represents the frequency dependence of the PSPWM power converter.

$\Delta\langle i_{\mathrm{LOut}}\rangle_N$ is a staircase function, where the amplitude changes at the beginning of every half switching cycle. $\Delta\langle i_{\mathrm{LOut}}\rangle_N$ is exactly the same as the continuous value $\Delta i_{\mathrm{LOut}}(t)$ averaged over a PSPWM converter half switching period, T. Fig. 8 shows the responses for a $\Delta v_{\mathrm{In}}u(t)$ perturbation. This instantaneous small-signal result uses the values from (25–30). The averaged waveform has the same average value (averaged over a half switching interval, T) as the exact instantaneous signal, but the averaged signal has a more abrupt amplitude step change. This creates a small high frequency mismatch between the gain and phase of the instantaneous and averaged responses.

F. PSPWM Converter Small-Signal Model

The PSPWM power converter dynamic behavior has some electrical properties best represented using discrete "z-transforms" and other continuous features best represented using Laplace or "s-transforms." It is important to merge these into a single electrical model. Traditional power converter small-signal models are represented in the s-domain. The sampled converter characteristics will be mapped into equivalent Laplace transforms to provide a complete s-domain representation of the PSPWM power converter small-signal model.

The PSPWM converter output filter includes a capacitor and load resistor (R_{Load}). These components are modeled using Laplace transforms. The dynamic averaged small-signal response of the PSPWM power converter includes the "$1-k^N$" term of (32). This "$1-k^N$" term is best represented using a discrete z-transform. It is important to remember that this "$1-k^N$" response results from a small-signal unit step perturbation. The "$1-k^N$" transfer function has the time response

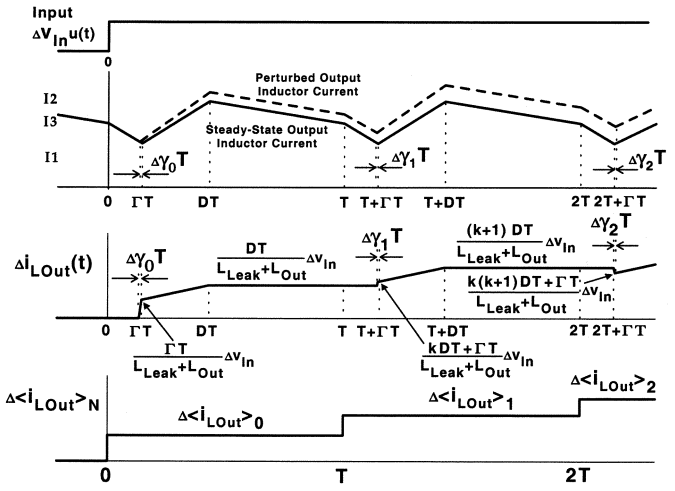

Fig. 8. Large signal, small-signal instantaneous (Δi_{LOut}), and small-signal averaged ($\Delta\langle i_{\mathrm{LOut}}\rangle_N$) output inductor current responses due to a small-signal input voltage step change, $\Delta v_{\mathrm{In}} u(t)$.

shown in Fig. 9, where the break "$\iint$" indicates that a long time has passed.

The Laplace transform of the function of Fig. 9 is

$$\boldsymbol{L}\left\{\sum_{N=0}^{\infty}(1-k^N)[u(t-NT)-u(t-\{N+1\}T)]\right\} = \frac{e^{-sT}(1-k)}{s(1-ke^{-sT})} \tag{33}$$

where "$\boldsymbol{L}\{\ldots\}$" means "the Laplace transform of."

While (33) is the s-domain representation for the staircase response, it is quite cumbersome. The complication is due to the "e^{-sT}" term. The model is simplified using the following first order Pade approximation

$$e^{-sT} \rightarrow \frac{\left(-s+\frac{2}{T}\right)}{\left(s+\frac{2}{T}\right)}. \tag{34}$$

Simplifying and substituting $k = (L_{\mathrm{Out}} - L_{\mathrm{Leak}})/(L_{\mathrm{Out}} + \mathrm{L_{Leak}})$ into the transfer function of "$1-k^N$" gives

$$\frac{e^{-sT}(1-k)}{(1-ke^{-sT})} \rightarrow \frac{-s+\frac{2}{T}}{\frac{L_{\mathrm{Out}}}{L_{\mathrm{Leak}}}s+\frac{2}{T}}. \tag{35}$$

Substituting the first order Pade approximation provides an s-domain small-signal model for the PSPWM power converter. Fig. 10 shows the PSPWM power converter small-signal model using the first order Pade approximation.

All necessary information for the small-signal averaged model of the PSPWM power converter has been calculated. The only other required information is the transfer function between the averaged small-signal output inductor current ($\Delta\langle i_{\mathrm{LOut}}\rangle_N$) and the small-signal output voltage (Δv_{Out}). This transfer function is simply the output capacitor and load in parallel. $Z_{\mathrm{Out}}(s)$ is the parallel impedance of the output filter capacitor, $Z_{Cap}(s)$, and load resistance, R_{Load}. The values of capacitor impedance, $Z_{Cap}(s)$, and output impedance, $Z_{\mathrm{Out}}(s)$, (output capacitor in parallel with load resistance) are

$$Z_{cap}(s) = \frac{1}{sC} \tag{36}$$

$$Z_{\mathrm{Out}}(s) = Z_{cap} \| R_{\mathrm{Load}} = \frac{R_{\mathrm{Load}}}{sCR_{\mathrm{Load}}+1}. \tag{37}$$

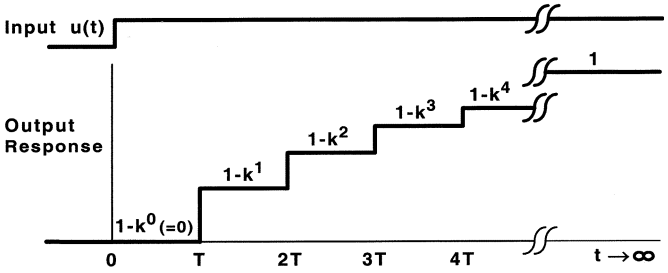

Fig. 9. Graph of input, $u(t)$, and piecewise constant staircase response.

The small-signal model of Fig. 10 is quite simple, yet provides an extremely accurate PSPWM power converter model. The converter has a high frequency zero. The effect of the converter dynamics upon the output L-C filter is significant. The output filter inductor (L_{Out}), leakage inductor (L_{Leak}), and switching frequency (T) became components of the "k" term discussed previously. The mathematical analysis showed that the output inductor became a constituent of the left-half plane pole at $(2L_{\mathrm{Leak}})/(TL_{\mathrm{Out}})$. The second real pole is due to the output capacitor in parallel with the load resistance. Thus, the output L-C filter is split into two real, distinct poles. The pole associated with the output inductor is constant and independent of input voltage, output voltage, and load resistance. All remaining terms in the small-signal model are simple constants that depend upon component values and dc operating conditions. There is a "feedforward path" for both the Δv_{In} and Δd small-signal inputs.

Fig. 10 has an added "Xfmr Turns Ratio" constant to account for the voltage gain due to a PSPWM power converter isolation transformer. This transformer turns ratio term, "Xfmr Turns Ratio," is necessary to properly model the small-signal output voltage on the secondary side of an isolation transformer. The transformer turns ratio is conventionally defined as the ratio of secondary side turns to primary side turns. For a center-tapped transformer the number of secondary side turns is the number of turns of each separate center-tapped winding, or half the total number of total secondary turns.

All constants in the model of Fig. 10 use parameters referenced to the primary side of the isolation transformer. All voltages and currents on the secondary side of the isolation transformer are scaled by the transformer turns ratio. Impedances on the secondary side are scaled by the square of the transformer turns ratio. Parameters on the secondary side of the isolation transformer use "primed" designators (e.g., $\Delta v'_{\mathrm{Out}}$). Parameters referenced to the transformer primary side use "nonprimed" designators (e.g., Δv_{Out}).

Both the forward gain and the feedforward path have gain terms of $T/(2L_{\mathrm{Leak}})$. The feedforward path has a constant multiplier of $(1-k)/2$. Since k is nearly unity ($L_{\mathrm{Leak}} \ll L_{\mathrm{Out}}$) for a well designed PSPWM power converter, these terms have a much smaller effect than the dominant frequency dependent forward gain term. Similarly, the forward gain term has a constant value of $1+\Gamma^2 L_{\mathrm{Leak}}/L_{\mathrm{Out}}$. Since $L_{\mathrm{Leak}} \ll L_{\mathrm{Out}}$ and $\Gamma \ll 1$, this constant is approximately one.

There is an output voltage feedback term in the small-signal model of Fig. 10. This modifies the phase-shifted PWM power converter output impedance.

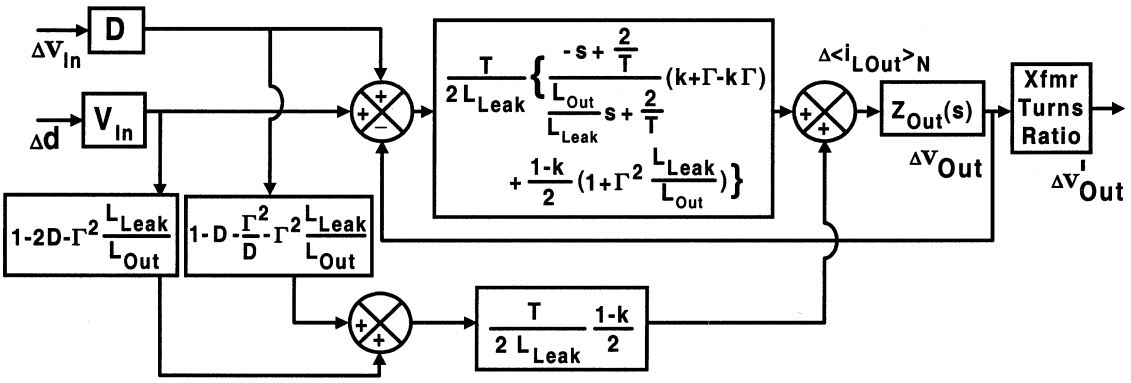

Fig. 10. Complete PSPWM power converter small-signal model.

The slew interval, Γ, increases with increasing load current. The voltage conversion ratio, $V_{\rm Out}/V_{\rm In}$, depends upon the input voltage, output voltage, inductor values, duty cycle, and load current. If inductor component values, duty cycle, and input voltage are all kept constant, then increasing load current maps to a reduced output voltage. Thus, the PSPWM power converter has a finite output impedance at low frequency.

The output impedance, Z_{PSPWM} is for the phase-shifted PWM power converter only, it does not include the load resistor, $R_{\rm Load}$. At low frequency ($s \to 0$) the PSPWM converter output impedance is

$$Z_{PSPWM-DC} = \frac{\frac{2L_{\rm Leak}}{T}}{1+(k-1)\left(\frac{1}{2}-\Gamma-\frac{\Gamma^2}{2}\frac{L_{\rm Leak}}{L_{\rm Out}}\right)}. \quad (38)$$

G. Small-Signal Input Current

The final parameter of interest is the averaged small-signal input current. This is required for calculating the resulting input current perturbations, especially due to input voltage disturbances. The ratio of small-signal input voltage to small-signal input current ($\Delta v_{\rm In}/\Delta i_{\rm In}$) is the PSPWM power converter small-signal input impedance. Using the same small-signal derivation approach as earlier gives the averaged small-signal response

$$\begin{aligned}&\Delta\langle i_{\rm In}(t)\rangle_N \\ &=\frac{T}{2L_{\rm Leak}}\{1-k^N\}\left\{Dk-\frac{2\Gamma L_{\rm Out}}{L_{\rm Leak}+L_{\rm Out}}\right\} \\ &\quad\times\{D\Delta v_{\rm In}-\Delta v_{\rm Out}+V_{\rm In}\Delta d\}+ \\ &\quad T\frac{(D^2+\Gamma^2\frac{L_{\rm Out}}{L_{\rm Leak}})\Delta v_{\rm In}-(D^2-\Gamma^2)\Delta v_{\rm Out}}{2(L_{\rm Leak}+L_{\rm Out})} \\ &\quad+\left\{\frac{\Gamma T}{2}\left(\frac{V_{\rm In}}{L_{\rm Leak}}+\frac{V_{\rm Out}}{L_{\rm Out}}\right)+\frac{V_{\rm Out}}{L_{\rm Leak}+L_{\rm Out}}(1-D)T\right\}\Delta d. \end{aligned} \quad (39)$$

The small-signal input current model is shown in Fig. 11.

IV. Experimental Results

A prototype phase-shifted PWM power converter was constructed to experimentally verify the small-signal model. Several small-signal measurements are performed using analog small-signal injection techniques. There is excellent agreement between the model and experimental measurements. The "primed" values in Fig. 12 (e.g., $v'_{\rm Out}$) represent the actual values on the secondary side of the center-tapped isolation transformer. The "nonprimed" values (e.g., $v_{\rm Out}$) represent the normalized values referenced to the transformer primary side. Fig. 13 is the small-signal model.

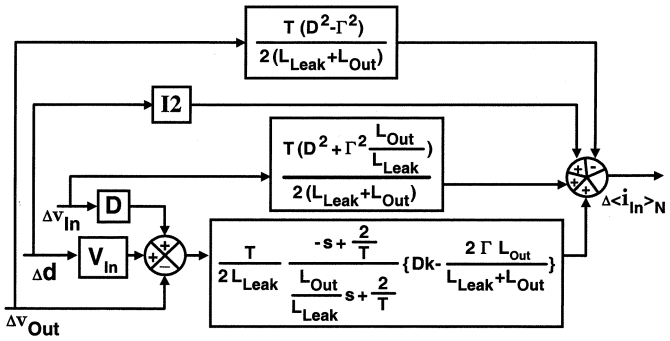

Fig. 11. Small-signal input current model.

The capacitor ESR has only a very minor effect upon the model presented earlier. The capacitor ESR creates a s-domain "zero" at 7.2 kHz. There is also a small capacitor equivalent series inductance (ESL) not included in the schematic.

Fig. 14 is the important control to output transfer function ($\Delta v'_{\rm Out}/\Delta d$). The experimental and model results are in excellent agreement, even up to half the switching frequency. The predicted pole at 19.7 kHz, due to the ratio of the inductors and switching frequency, corresponds well with measured results. The phase of the small-signal model and experimental converters is less accurate at higher frequencies because the averaged model assumes a "step-change" in amplitude at the start of every switching interval, and it also includes the Pade approximation. Still, the experimental measurement differs from the small-signal model by only 25° at half the switching frequency.

Fig. 15 is the measured and predicted PSPWM converter audio susceptibility ($\Delta v'_{\rm Out}/\Delta v_{\rm In}$). There is again excellent agreement between the model and experimental results. The frequency range for this measurement is 5 Hz to 50 kHz. This frequency range is limited by the signal injection transformers required to perform this measurement.

Fig. 16 shows the measured and predicted PSPWM converter output impedance, Z_{PSPWM}. At low frequencies

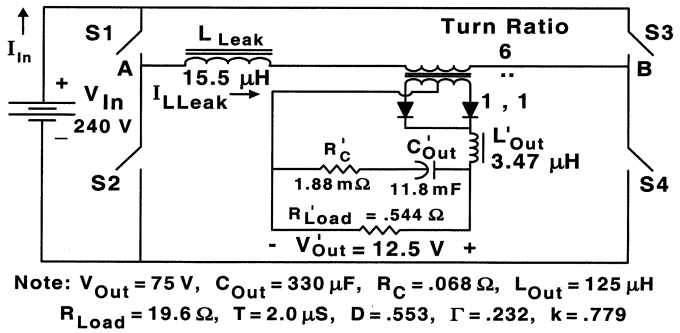

Fig. 12. Schematic of PSPWM power converter.

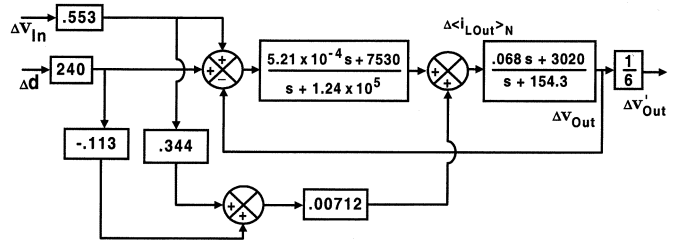

Fig. 13. Small-signal model for PSPWM power converter of Fig. 12.

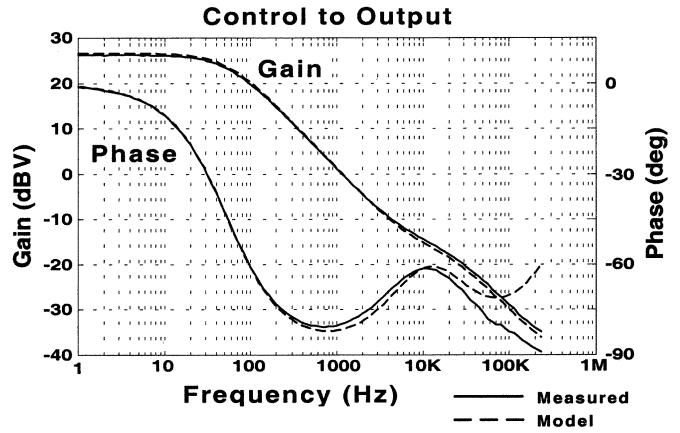

Fig. 14. PSPWM converter control to output: measured result and small-signal model.

(up to approximately 30 Hz) the output impedance is constant, then a pole occurs. The output impedance at dc, from (38) is 16.46 $\Omega/6^2$ (.46 Ω), or -6.8 dBΩ. This agrees extremely well to the measured dc output impedance of 0.48 Ω (-6.4 dBΩ). Above 100 Hz the output impedance is dominated by the output capacitance.

Fig. 17 is the measured and predicted PSPWM converter input impedance. This is the ratio of small-signal input voltage to small-signal input current ($\Delta v_{\rm In}/\Delta i_{\rm In}$). This is a difficult measurement to perform. There is a large high frequency circulating input current for the PSPWM converter, complicating the measurement. Performing this measurement requires adding a high frequency decoupling capacitance close to the input of PSPWM converter H-bridge. There is 1.2 μF of high frequency decoupling capacitance included in the input impedance measurement. Both the theoretical and experimental input impedances include 1.2 μF of input capacitance. This additional high frequency decoupling capacitance creates a "pole" at 660 Hz.

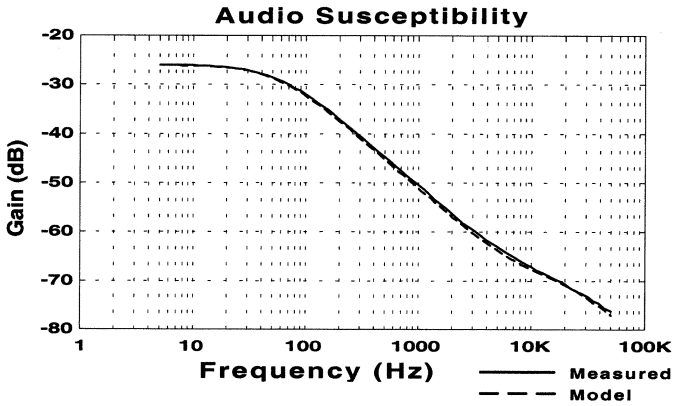

Fig. 15. PSPWM converter audio susceptibility: measured result and small-signal model.

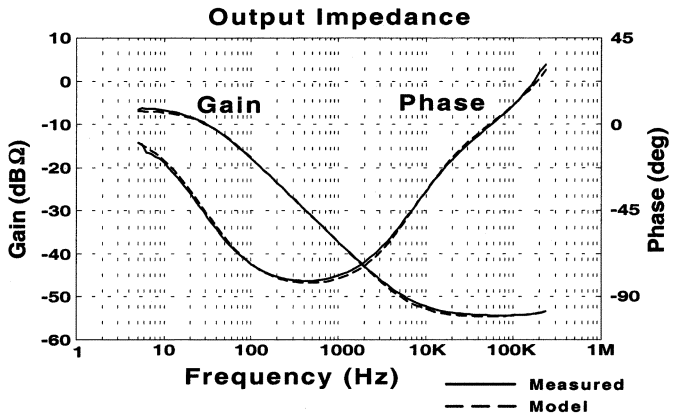

Fig. 16. PSPWM converter output impedance: measured result and small-signal model.

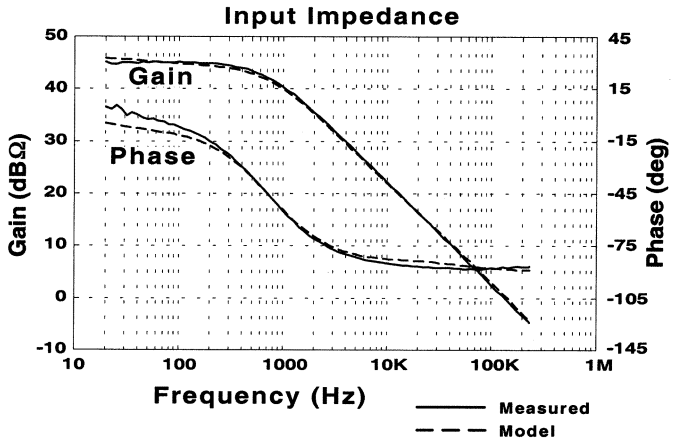

Fig. 17. PSPWM converter input impedance: measured result and small-signal model. Includes 1.2 μF input capacitance.

V. Conclusion

Conventional small-signal derivation techniques do not properly model the PSPWM power converter due to the complex and implicit slew interval dynamics. A small-signal technique is presented which derives the PSPWM power converter natural

and forced responses, then solves for the generalized response at any time after the introduction of a small-signal input perturbation. The resulting small-signal model uses the instantaneous small-signal currents of the perturbed system. Cycle by cycle averaging is performed using the exact small-signal response equations. Since complete high frequency dynamic information is maintained until averaging, an accurate high frequency small-signal model results. This model provides a simple, extremely accurate representation for the dynamics associated with the PSPWM power converter. This model provides the exact averaged small-signal dynamics associated with the PSPWM power converter. The PSPWM converter model shows that the output L-C filter is separated into two real poles, with one pole at a constant frequency independent of operating conditions. The small-signal model is in excellent agreement with experimental measurements.

REFERENCES

[1] R. A. Fisher, K. D. T. Ngo, and M. H. Kuo, "A 500 kHz, 250 W dc-dc converter with multiple outputs controlled by phase-shifted PWM and magnetic amplifiers," in *Proc. High Freq. Power Conv. Conf.*, 1988, pp. 100–110.

[2] J. A. Sabate, V. Vlatkovic, R. Ridley, F. C. Lee, and B. H. Cho, "Design considerations for high-voltage high-power full-bridge zero-voltage-switched PWM converter," *Proc. IEEE APEC'90 Conf.*, pp. 275–284, 1990.

[3] M. J. Schutten, M. H. Kheraluwala, R. L. Steigerwald, and D. A. Torrey, "EMI comparison of hard switched, edge-resonant, and load resonant dc/dc converters using a common power stage," *Proc. IEEE IAS'98 Conf.*, pp. 1588–93, 1998.

[4] V. Vlatkovic, J. A. Sabate, R. B. Ridley, F. C. Lee, and B. H. Cho, "Small-signal analysis of zero-voltage switched full-bridge PWM converter," in *Proc. High Freq. Power Conv. Conf.*, 1990, pp. 262–272.

[5] M. J. Schutten, "Operation and control characteristics of a zero-voltage transition PWM power converter," Ph.D. dissertation, Rensselaer Polytech. Inst., Troy, NY, 2000.

[6] R. W. Erickson, *Fundamentals of Power Electronics*. New York: Chapman and Hall, 1997.

[7] D. B. Dalal, "A 500-kHz multi-output converter with zero voltage switching," *Proc. IEEE APEC'90 Conf.*, pp. 265–274, 1990.

Michael Schutten (M'83) received the B.S. and M.S. degrees in electrical engineering from Marquette University, Milwaukee, WI, and the M.S. and Ph.D. degrees in electric power engineering from Rensselaer Polytechnic Institute, Troy, NY.

From 1983 to 1987, he worked for General Electric Medical Systems where he developed high frequency X-ray and CT generators. For the last 15 years he has been a Member of Technical Staff, General Electric Global Research Center, Niskayuna, NY. He has developed several high density, low noise power converters for commercial, industrial, and military applications. His research includes high performance power conversion with an emphasis on advanced converter topologies and novel electromagnetic compatibility approaches. His areas of expertise include power converter topologies, electromagnetic interference, soft-switching conversion, high frequency magnetics, nonlinear control theory, and analog electronics. He has 13 issued patents, with several additional pending. He has authored several conference and transactions papers.

Dr. Schutten is a member of Tau Beta Pi, Eta Kappa Nu, and the IEEE Power Electronics Society.

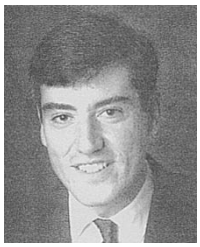

David A. Torrey (M'95) received the B.S. degree in electrical engineering from Worcester Polytechnic Institute, Worcester, MA, and the S.M., E.E., and Ph.D. degrees in electrical engineering from the Massachusetts Institute of Technology, Cambridge.

He spent 14 years in academia with faculty appointments at Worcester Polytechnic Institute (then Rensselaer Polytechnic Institute, Troy, NY), where he held the Niagara Mohawk Power Electronics Research Chair. His research activities are focused on all aspects of electric machine systems, with emphasis on switched reluctance and brushless dc technology. He is now a Principal with Advanced Energy Conversion, LLC (a consulting firm focused on product development that integrates electric machines, power electronics, and embedded controls).

Dr. Torrey is a member of Sigma Xi, Tau Beta Pi, and Eta Kappa Nu. He has been involved in IEEE activities which support power electronics through the Applied Power Electronics Conference. He is a Registered Professional Engineer in New York State.